

Bis[2-(4'-Bromopyrazolyl-1')-3-Tosylaminopyridinato]zinc(II): Synthesis, Structure, and Luminescence Properties

A. S. Burlov^{a,*}, Yu. V. Koshchienko^a, V. G. Vlasenko^b, A. A. Zubenko^c, M. A. Kiskin^d, A. V. Dmitriev^e,
E. I. Mal'tsev^e, D. A. Lypenko^e, S. A. Nikolaevskii^{a, d}, and D. A. Garnovskii^{a, f}

^a Research Institute of Physical and Organic Chemistry, Southern Federal University, Rostov-on-Don, Russia

^b Research Institute of Physics, Southern Federal University, Rostov-on-Don, Russia

^c North Caucasian Regional Research Veterinary Institute, Novocherkassk, Russia

^d Kurnakov Institute of General and Inorganic Chemistry, Russian Academy of Sciences,
Leninskii pr. 31, Moscow, 119991 Russia

^e Frumkin Institute of Physical Chemistry and Electrochemistry, Russian Academy of Sciences,
Leninskii pr. 31, Moscow, 119991 Russia

^f Southern Scientific Center, Russian Academy of Sciences, Rostov-on-Don, Russia

*e-mail: anatoly.burlov@yandex.ru

Received November 6, 2013

Abstract—2-(4'-Bromopyrazolyl-1')-3-tosylaminopyridine (HL^3) and its complex ZnL_2 (**I**) are synthesized, and their structures are studied by IR, UV, and 1H NMR spectroscopy. The molecular structure of complex ZnL_2 is determined by X-ray diffraction analysis. The atomic structure of ZnL_2 is confirmed by the optimization of the molecular geometry using quantum-chemical calculations in the density functional theory approximation. The experimental bands in the absorption spectrum of complex **I** are interpreted on the basis of the calculations, and its photoluminescence properties are studied.

DOI: 10.1134/S1070328414080016

INTRODUCTION

Heterocyclic compounds capable of forming chelate structures with coordination spheres MN_4 , MN_4O_2 , and MN_2S_2 ($M = Zn, Cd$) attract much interest due to the possibility to obtain metal complexes with photo- and electroluminescence properties. Practical importance of these metal chelates is the use of such compounds as emitting layers in organic light emitting diodes (OLED) and also as electron-transport layers in these devices. Metal chelates luminescing in the blue spectral range, for example, the zinc complexes with 7-azaindoles [1–3], di-2-pyridylamine, 2,6-bis(2-pyridylamino)pyridine [4], 2,6-bis(benzimidazolyl)pyridine [5, 6], 1,3,4-oxadiazole, 2-(2'-hydroxyphenyl)-5-phenyl-1,3-oxadiazole [7], and 2-(2'-hydroxyphenyl)-2-oxazoline [8], which is rarely met for standard inorganic luminophores.

The OLED devices were produced in which the heterocyclic zinc(II) complexes with 2-(2'-hydroxyphenyl)benzimidazole [9–11], 2-(2'-hydroxyphenyl)benzoxazole [12–14], 2-(2'-hydroxyphenyl)benzothiazole [15–20], and 2-(2'-tosylaminophenyl)benzoxazole [21, 22] were used as electroluminescent layers. These complexes are resistant to the exposure,

light, and temperature. They are synthetically accessible, have suitable photoluminescent (PL) and electroluminescent (EL) properties, can be readily modified for optimization of characteristics, and form homogenous thin films upon vacuum thermal evaporation.

However, an information about the electronic structures of the complexes is very important, along with the structure, photophysical properties, thermal stability, and volatility, for the development of new electroluminescent layers in OLED. One of criteria for the selection of materials for the production of OLED is the correspondence of the work functions of the electrode materials to the positions of the HOMO (highest occupied molecular orbital) and LUMO (lowest unoccupied molecular orbital) of the substance of the active electroluminescent layer [23–25].

In this work, the data on the synthesis, X-ray diffraction analysis, and photoluminescence properties of the bis[2-(4'-bromopyrazolyl-1')-3-tosylaminopyridinato]zinc(II) complex (ZnL_2 , **I**) are presented. The experimental results and the data on the electronic structure of ZnL_2 were compared to the quan-

tum-chemical calculation data in the density functional theory (DFT) approximation.

EXPERIMENTAL

Commercially accessible (Aldrich) 2-chloro-3-nitropyridine, 4-bromopyrazole, and *p*-toluenesulfonyl chloride were used.

Synthesis of 2-(4'-bromopyrazolyl-1')-3-nitropyridine (L¹). Sodium hydride (60%, 4.0 g, 0.1 mol) was added by portions of 0.5 g with cooling and stirring in a nitrogen atmosphere to a solution of 4-bromopyrazole (14.7 g, 0.1 mol) in anhydrous DMF (60 mL), maintaining the temperature of the reaction mixture lower than 10°C. The mixture was stirred for 1 h at room temperature, 2-chloro-3-nitropyridine (15.8 g, 0.1 mol) was added on cooling by portions of 0.5 g, and the mixture was stirred for 30 min and poured into water (300 mL). The precipitate was filtered off, washed with water, and dried. The yield was 16.2 g (60%). The product was recrystallized from ethanol, mp = 132–133°C; according to [26], mp = 133–134°C.

¹H NMR (DMSO-d₆; δ, ppm: 7.63 (1H, q, *J* = 4.8 Hz, H⁵_{pyridine}), 7.70 (1H, s, H³_{pyrazole}), 8.39 (1H, dd, *J* = 8.1 Hz, *J* = 1.5 Hz, H⁶_{pyridine}), 8.57 (1H, s, H⁵_{pyrazole}), 8.67 (1H, dd, *J* = 4.8 Hz, *J* = 1.5 Hz, H⁴_{pyridine}).

Synthesis of 2-(4'-bromopyrazolyl-1')-3-aminopyridine (H₂L²). A mixture of ethanol (200 mL), powdered iron (30 g), and concentrated hydrochloric acid (5 mL) was refluxed with stirring for 1 h. Ligand L¹ (26.9 g, 0.1 mol) was added by portions of 2 g for 2 h to the boiling reaction mixture with vigorous stirring, and the mixture was refluxed for additional 3 h. Powdered potassium carbonate (12 g) was added by portions of 1 g to the boiling mixture. The mixture was refluxed for 30 min and filtered. The solution was reduced to a volume of 100 mL, and an excess of an alcohol solution of hydrochloric acid was added with stirring. 2-(4'-Bromopyrazolyl-1')-3-nitropyridine hydrochloride that formed was filtered off and treated with a 22% solution of ammonia. The yield was 12.9 g (54%). The beige-colored crystals with mp = 108–109°C were obtained.

For C₈H₇N₄Br

anal. calcd., %: C, 40.19; H, 2.95; N, 23.44.
Found, %: C, 40.15; H, 3.04; N, 23.47.

¹H NMR (DMSO), δ, ppm: 6.25 (2H, s, NH₂), 7.02 (1H, q, *J* = 4.5 Hz, H⁵_{pyridine}), 7.25 (1H, d, *J* = 7.8 Hz, H⁶_{pyridine} or H⁴_{pyridine}), 7.62 (1H, d, *J* = 3.6 Hz,

H⁴_{pyridine} or H⁶_{pyridine}), 7.69 (1H, s, H³_{pyrazole}), 8.55 (1H, s, H⁵_{pyrazole}). IR, ν, cm^{−1}: 3412 ν_{as}(NH₂), 3290 ν_s(NH₂), 1614 δ(NH₂).

Synthesis of 2-(4'-bromopyrazolyl-1')-3-tosylaminopyridine (HL³). A mixture of H₂L² (2.39 g, 0.01 mol), *p*-toluenesulfonyl chloride (1.91 g, 0.01 mol), and sodium acetate trihydrate (1.36 g, 0.01 mol) in ethanol (10 mL) was refluxed for 2 h and cooled. The precipitate was filtered off, washed with ethanol and water, and dried. Then the precipitate was dissolved in chloroform and passed through an alumina layer. The solvent was distilled off, and beige crystals with mp = 132–133°C were obtained. The yield was 3.11 g (79%).

For C₁₅H₁₃N₄O₂SBr

anal. calcd., %: C, 45.81; H, 3.33; N, 14.25.
Found, %: C, 45.72; H, 3.41; N, 14.29.

¹H NMR (DMSO-d₆), δ, ppm: 2.30 (3H, s, CH₃), 7.23 (2H, d, *J* = 8.1 Hz, H³_{phenyl} and H⁵_{phenyl}), 7.43–7.46 (3H, m, H⁵_{pyridine}, H²_{phenyl}, and H⁶_{phenyl}), 8.00 (1H, d, *J* = 8.1 Hz, H⁴_{pyridine}), 8.07 (1H, s, H⁵_{pyrazole}), 8.26 (1H, d, *J* = 3.6 Hz, H⁶_{pyridine}), 8.50 (1H, s, H³_{pyrazole}), 10.59 (1H, s, NH). IR, ν, cm^{−1}: 3153 ν(NH), 1334 ν_{as}(SO₂), 1166 ν_s(SO₂).

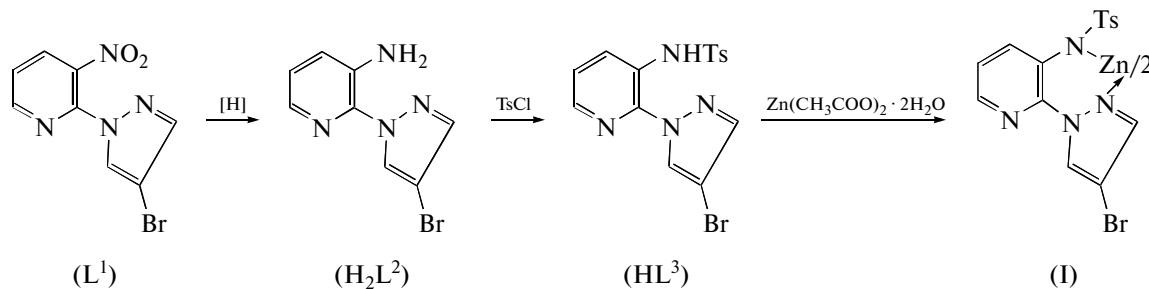
Synthesis of complex I. A solution of zinc acetate dihydrate (92 mg, 0.5 mmol) in ethanol (3 mL) was poured to a solution of HL³ (393 mg, 1 mmol) in ethanol (6 mL), and the mixture was refluxed for 2 h. After cooling, the precipitate that formed was filtered off, washed with ethanol, and dried. The yield was 292 mg (69%). The product was recrystallized from acetonitrile, and colorless crystals with mp > 300°C were obtained.

For C₃₀H₂₄N₈O₄S₂Br₂Zn

anal. calcd., %: C, 42.40; H, 2.85; N, 13.18; Zn, 7.69.
Found, %: C, 42.29; H, 2.94; N, 13.25; Zn, 7.80.

¹H NMR (DMSO-d₆), δ, ppm: 2.27 (6H, s, 2CH₃), 7.13–7.18 (8H, m, H⁴_{pyridine}, H⁵_{pyridine}, H³_{phenyl}, and H⁵_{phenyl}), 7.51 (4H, br.s, H²_{phenyl} and H⁶_{phenyl}), 7.75 (2H, d, *J* = 7.2 Hz, H⁶_{pyridine}), 8.03 (2H, s, H⁵_{pyrazole}), 10.06 (2H, br.s, H³_{pyrazole}). IR, ν, cm^{−1}: 1271 ν_{as}(SO₂), 1136 ν_s(SO₂).

The synthesis of complex I is shown in the scheme



IR spectra were recorded on a Varian 3100-FTIR Excalibur instrument in powders by the frustrated total internal reflectance method. ^1H NMR spectra were measured on a Varian Unity-300 instrument (300 MHz) in the internal stabilization mode at the ^2H polar line in DMSO-d_6 .

Absorption spectra were recorded on Varian Cary 1E and UNICAM Helios Gamma spectrophotometers in toluene solutions. Photoluminescence spectra were detected on a Varian Cary Eclipse lattice spectrofluorimeter (spectral range from 200 to 800 nm, photoexcitation wavelength 380 nm).

The X-ray diffraction analysis of complex **I** was carried out¹ on a Bruker SMART APEX II diffractometer equipped with a CCD detector and a monochromatic radiation source (MoK_α , $\lambda = 0.71073 \text{ \AA}$) using a standard procedure [27]. A semiempirical absorption correction was applied [28]. The structure was solved by a direct method and refined in the full-matrix least-square anisotropic approximation for all non-hydrogen atoms. The hydrogen atoms at the carbon atoms of the organic ligands were specified geometrically and refined in the rider model. The calculations were performed according to the SHELXS-97 and SHELXL-97 programs [29]. The crystallographic parameters of complex **I** are the following: $\text{FW} = 849.88$, crystal size $0.15 \times 0.10 \times 0.10 \text{ mm}$, colorless, prismatic, $T = 173(2) \text{ K}$, triclinic crystal system $P\bar{1}$, $a = 9.779(11)$, $b = 11.063(13)$, $c = 16.341(19) \text{ \AA}$, $\alpha = 88.273(17)^\circ$, $\beta = 79.556(18)^\circ$, $\gamma = 71.376(16)^\circ$, $V = 1647(3) \text{ \AA}^3$, $Z = 2$, $\rho = 1.714 \text{ g/cm}^3$, $\mu = 3.348 \text{ mm}^{-1}$, $\theta = 2.23^\circ - 27.0^\circ$, $-12 \leq h \leq 12$, $-14 \leq k \leq 14$, $-20 \leq l \leq 20$; total number of reflections 15377, independent reflections 7149, reflections with $I \geq 2\sigma(I)$ 4625, $R_{\text{int}} = 0.0741$, $T_{\text{min}}/T_{\text{max}} = 0.6336/0.7307$, $S = 0.920$, $R_1 = 0.0949$, $wR_2 = 0.1577$ (for all data), $R_1 = 0.0605$, $wR_2 = 0.1446$

¹ The X-ray diffraction analysis was carried out at the Center for Collective Use of the Kurnakov Institute of General and Inorganic Chemistry, Russian Academy of Sciences.

(for $I \geq 2\sigma(I)$), $\Delta\rho_{\text{min}}/\Delta\rho_{\text{max}} = -1.550/1.704 \text{ e \AA}^{-3}$. The full array of X-ray diffraction data was deposited with the Cambridge Crystallographic Data Centre (no. 965634; deposit@ccdc.cam.ac.uk or http://www.ccdc.cam.ac.uk/data_request/cif).

The geometry of molecule **I** in the ground state was calculated using the GAUSSIAN03 program [30] in the DFT approximation. The hybrid three-parametric B3LYP functional [31, 32] and standard split-valence polarized 6-31G(d) basis set [33, 34] were chosen for the calculations. This calculation scheme was several times and successfully used for molecular structure optimization for both organic compounds and metal complexes.

The absorption spectra in the UV and visible ranges for molecules were calculated in the framework of the time-dependent DFT-TD-DFT nonstationary density functional theory using optimized parameters of the atomic structure and taking into account the solvent (toluene) effect. The forms of the functional and basis set for the calculation of the absorption spectra were chosen to be the same as those for the molecular geometry calculation.

RESULTS AND DISCUSSION

According to the IR and ^1H NMR spectral data, ligand HL^3 exists in the aminopyridine tautomeric form both in the solution and solid state. This is confirmed by a broadened singlet in the ^1H NMR spectrum of HL^3 at 10.59 ppm (proton of the NH group) and the stretching vibration band at 3153 cm^{-1} in the IR spectrum. On going to the spectra of complex **I**, the corresponding signals disappear, indicating the deprotonation of the tosylated amino group and complex formation.

The X-ray diffraction of compound **I** revealed that the aminopyridine tautomeric form is retained upon complex formation with the Zn^{2+} ion (Fig. 1). The bond lengths in the ligand (the main structure charac-

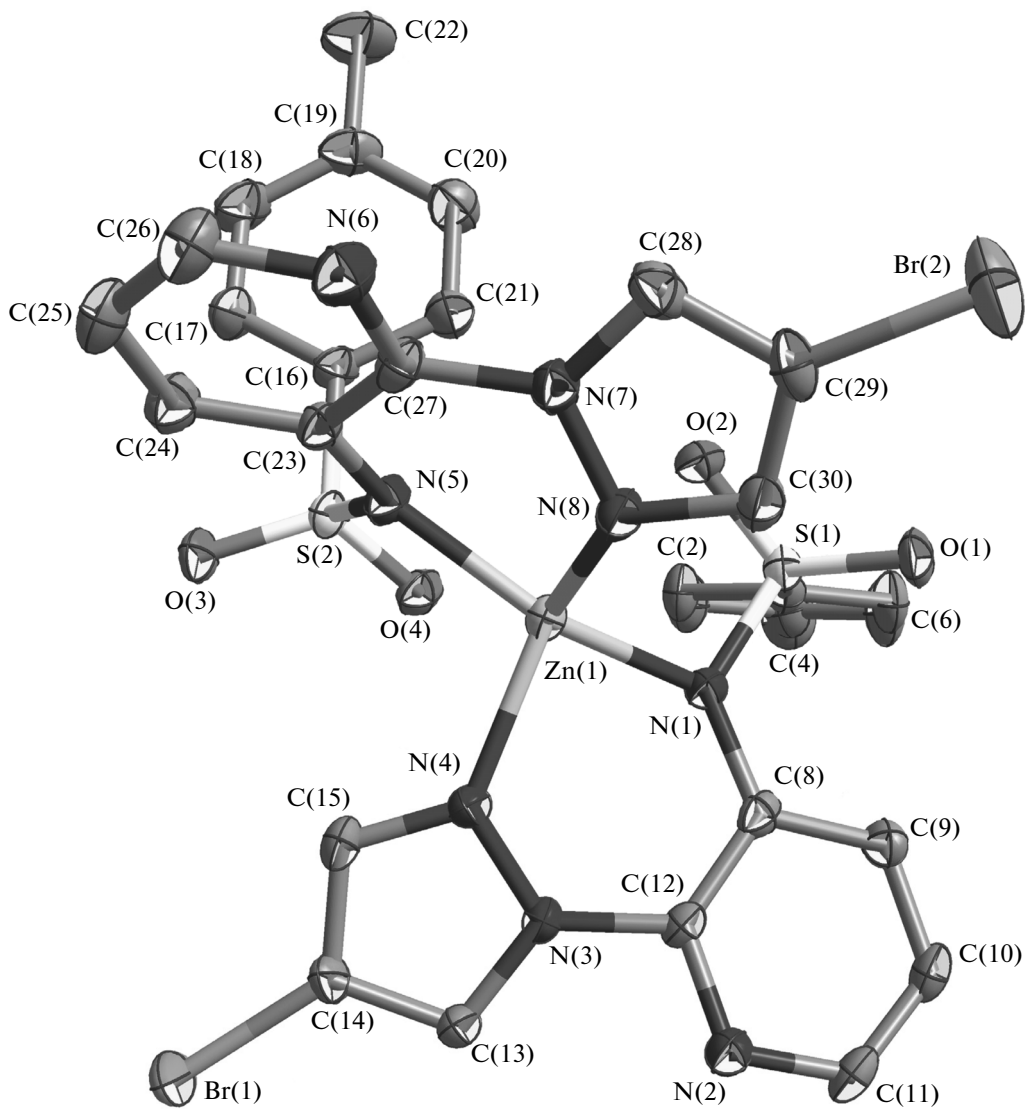


Fig. 1. Molecular structure of complex I according to the X-ray diffraction data (hydrogen atoms are omitted, thermal ellipsoids with 50% probability).

teristics are given in Table 1) corresponds to the known bond lengths in the structurally characterized pyrazolypyridines [35]. The N(3)–N(4) and N(7)–N(8), C(13)–N(3) and C(28)–N(7), and C(15)–N(4) and C(30)–N(8) bond lengths range in the known ranges: 1.35–1.38, 1.33–1.38, and 1.31–1.34 Å, respectively. At the same time, the C(12)–N(3) and C(27)–N(7) bonds are elongated compared to the known (1.40–1.42 Å) values [35].

Two molecules of monodeprotonated compound HL^3 are coordinated to the central zinc atom through the chelate mode and act as bidentate N,N -ligands (Fig. 1). The central zinc atom is in the distorted tetrahedral environment of four N atoms. The value of

the N(5)Zn(1)N(1) angle is 152.19(17)°, which most strongly deviates from the value ideal for a tetrahedron (109.5°). The chelate rings are nonplanar, and the angle between the planes N(1)Zn(1)N(4) and N(5)Zn(1)N(8) is 66.4(2)°. The Zn(1) atom shifts from the N(1)N(3)N(4) and N(5)N(7)N(8) planes by 0.304(1) and 0.235(1) Å, respectively. The C(8), C(12) and C(23), C(27) atoms shift from these planes by 0.214(5), 0.284(5) and 0.695(5), 0.666(5) Å, respectively. The planes of the pyrazole and pyridine rings C(13)–N(4) and C(9)–N(2)C(12) are inclined to each other by 22.0(2)°. In the adjacent chelate fragment, the angle between the planes of similar rings C(28)–N(7) and C(23)–N(6)C(27) is 32.9(2)°.

Table 1. Selected bond lengths d (Å) and bond angles ω (deg) in molecule **I** according to the data of X-ray diffraction analysis and quantum-chemical calculations

Bond	d , Å	
	X-ray diffraction analysis	theory
N(3)–N(4)	1.375(5)	1.360(3)
N(7)–N(8)	1.370(5)	1.360(2)
C(12)–N(3)	1.444(6)	1.438(8)
C(13)–N(3)	1.358(6)	1.361(1)
C(15)–N(4)	1.329(6)	1.334(9)
C(27)–N(7)	1.433(6)	1.438(7)
C(28)–N(7)	1.360(6)	1.361(1)
C(30)–N(8)	1.332(6)	1.334(8)
Zn(1)–N(1)	2.000(4)	1.990(5)
Zn(1)–N(4)	2.031(4)	2.070(8)
Zn(1)–N(5)	1.987(4)	1.990(2)
Zn(1)–N(8)	2.079(5)	2.070(5)
Angle	ω , deg	
	X-ray diffraction analysis	theory
O(1)S(1)N(1)	113.3(2)	113.4(4)
O(3)S(2)N(5)	113.9(2)	113.4(3)
O(1)S(1)C(1)	107.6(2)	107.5(8)
O(2)S(1)C(1)	107.6(2)	108.5(1)
O(3)S(2)C(16)	107.5(2)	107.5(7)
O(4)S(2)C(16)	108.2(2)	108.5(6)
C(1)S(1)N(1)	107.6(2)	107.2(1)
C(16)S(2)N(5)	107.3(2)	107.1(4)
N(1)Zn(1)N(4)	89.33(17)	88.65(8)
N(1)Zn(1)N(5)	152.19(17)	155.44(3)
N(1)Zn(1)N(8)	104.14(16)	104.11(6)
N(4)Zn(1)N(5)	104.50(18)	103.97(2)
N(4)Zn(1)N(8)	121.48(17)	117.63(5)
N(5)Zn(1)N(8)	89.25(16)	88.77(1)

The S(1) and S(2) atoms in the tosyl fragments are characterized by the distorted tetrahedral environment of the O(1), O(2), O(3) and O(4), N(1), and N(5) atoms of the secondary amino group and the C(1) and C(17) atoms of the phenyl rings, respectively. The angles O(1)S(1)O(2), O(3)S(2)O(4) and O(2)S(1)N(1), O(4)S(2)N(5), whose values are 117.1(2)°, 116.8(2)° and 103.3(2)°, 102.6(2)°, respectively, deviate from tetrahedral angles most appreciably. The nearest to the central zinc ion oxygen atoms of the SO₂ groups are arranged at nonbonding distances Zn(1)…O(2) and Zn(1)…O(4) equal to 2.673(4) and 2.619(4) Å, respectively.

The phenyl rings of the aldehyde fragments C(1)–C(6) and C(16)–C(21) are arranged to the pyridine rings C(8)–N(2)C(12) and C(23)–N(6)C(27) at angles of 81.4(2)° and 81.4(2)°, respectively. A similar angle (81.85(6)°) was earlier observed between two phenyl rings in a 2-tosylaminobenzaldehyde molecule [36].

As follows from the data in Table 1, the obtained optimized parameters for the molecular structure of the complex are consistent with the experimental data (the maximum deviation for the distances is 4%, and that for the angles is 0.5%).

The main absorption bands in the theoretical UV spectra of complex **I** differed from the experimental values by several nm (Fig. 2, Table 2), which also confirms that the calculation of the optimized molecular structure is valid. The intense electronic transitions in the spectra mainly correspond to the ligand-to-ligand charge transfer of the π – π^* type. The longest-wavelength absorption band (320 nm) corresponds to the electronic transition HOMO → LUMO (Fig. 3) from which it follows that the electron density in the HOMO and LUMO is mainly localized on the pyrazolyl fragment of the ligand. However, a significant part of the electron density in the HOMO falls onto the nitrogen atom of the tosylamine fragment, while the electron density in the LUMO is not localized on this atom.

The photoluminescence spectrum of complex **I** in a toluene solution is also shown in Fig. 2. The photoluminescence band maximum appears at 384 nm and undergoes a bathochromic shift toward the long-wavelength absorption maximum by 64 nm. The photoluminescence quantum yield of complex **I** is ~0.04.

Complex **I** was used as an emission layer in the OLED device. However, the electroluminescence spectrum was not detected because of the low intensity to 16–17 V.

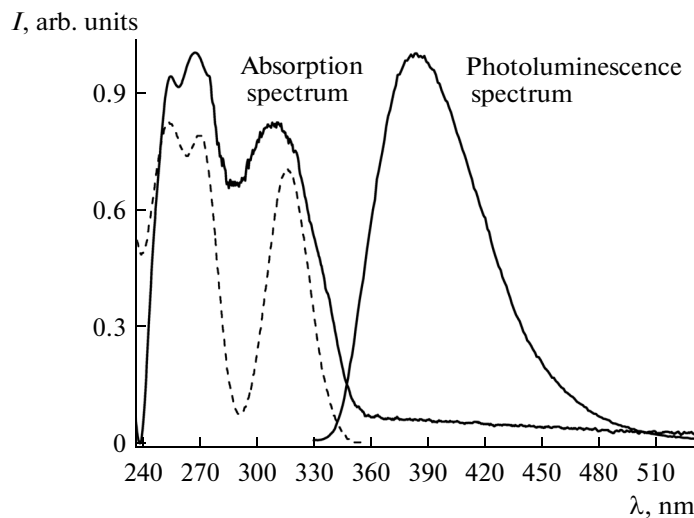


Fig. 2. (Solid line) experimental and (dashed line) theoretical absorption spectra and (solid line) the photoluminescence spectrum of complex **I**.

Table 2. Wavelengths of the main vertical electronic transitions (λ), energies (E), oscillator forces (f), and absorption band assignments to electronic transitions and their contributions for complex **I** calculated by the TD-DFT method

λ , nm	E , eV	Electronic transitions and their contributions, %	f
321.5 (320)*	3.857	HOMO \rightarrow LUMO	86.0
313.2 (310)	3.958	HOMO-1 \rightarrow LUMO+1 HOMO \rightarrow LUMO+1	47.6 43.0
273.5 (275)	4.534	HOMO \rightarrow LUMO+2 HOMO \rightarrow LUMO+3	13.8 72.8
270.8 (268)	4.579	HOMO-1 \rightarrow LUMO+2 HOMO \rightarrow LUMO+2	55.8 21.8
257.7 (254)	4.812	HOMO-3 \rightarrow LUMO	73.7
248.6	4.987	HOMO-5 \rightarrow LUMO HOMO-4 \rightarrow LUMO+1 HOMO-1 \rightarrow LUMO+4 HOMO \rightarrow LUMO+5	12.6 19.2 15.2 27.6

* Experimental values.

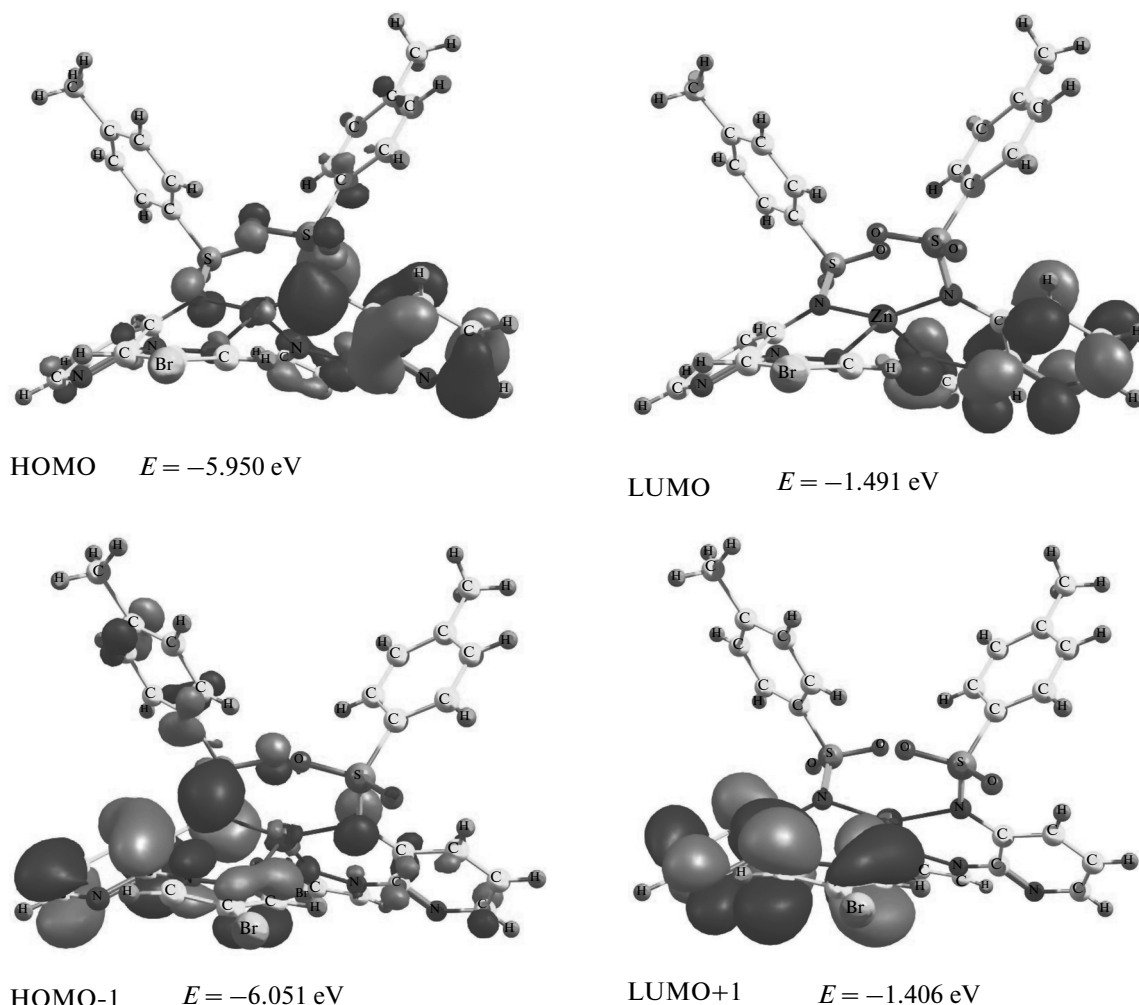


Fig. 3. Frontier molecular orbitals of complex I and their energies.

ACKNOWLEDGMENTS

This work was supported by the President of the Russian Federation (grant no. NSh-274.2014.3) and the Russian Foundation for Basic Research (project nos. 12-03-00462a and 13-03-00171a).

REFERENCES

1. Lee, C.F., Chin, K.F., Peng, S.M., and Che, C.M., *J. Chem. Soc., Dalton Trans.*, 1993, p. 467.
2. Ma, Y.G., Chao, H.Y., Wu, Y., et al., *Chem. Commun.*, 1998, p. 2491.
3. Ma, Y.G., Lai, T.S., and Wu, Y., *Adv. Mater.*, 2000, vol. 12, no. 6, p. 433.
4. Ho, K.Y., Yu, W.Y., Cheung, K.K., and Che, C.M., *Dalton Trans.*, 1999, p. 1581.
5. Liu, S.G., Zuo, J.L., Wang, Y., et al., *J. Phys. Chem. Solids*, 2005, vol. 66, no. 5, pp. 735.
6. Yue, S.M., Xu, H.B., Ma, J.F., et al., *Polyhedron*, 2006, vol. 25, no. 3, p. 635.
7. Kim, T.S., Okubo, T., and Mitani, T., *Chem. Mater.*, 2003, vol. 15, no. 26, p. 4949.
8. Zhang, J., Gao, S., and Che, C.M., *Eur. J. Inorg. Chem.*, 2004, vol. 2004, no. 5, p. 956.
9. Xu Hui, Xu Zhi-Feng, Yue Zheng-Yu, et al., *J. Phys. Chem., C*, 2008, vol. 112, no. 39, p. 15517.
10. Tong, Y.P., Zheng, S.L., and Chen, X.M., *Eur. J. Inorg. Chem.*, 2005, vol. 2005, no. 18, p. 3734.
11. Tong, Y.P., Zheng, S.L., and Chen, X.M., *J. Mol. Struct.*, 2006, vol. 826, nos. 2–3, p. 104.
12. Nakamura, N., Wakabayashi, S., Miyairi, K., and Fujii, T., *Chem. Lett.*, 1994, vol. 23, no. 9, p. 1741.
13. Yakushenko, I.K., Kaplunov, M.G., and Krasnikova, S.S., RF Pat. 2368641, *Byull. Izobret.*, 2009, no. 27.
14. Rai, V.K., Srivastava, R., and Kamalasan, M.N., *Synth. Met.*, 2009, vol. 159, no. 3, p. 234.
15. Li, Z., Dellali, A., Malik, J., et al., *Inorg. Chem.*, 2013, vol. 52, no. 3, p. 1379.
16. Yu, G., Yin, S., Liu, Y., et al., *J. Am. Chem. Soc.*, 2003, vol. 125, no. 48, p. 14816.

17. Qureshi, M., Manoharan, S.S., Singh, S.P., et al., *Solid State Commun.*, 2005, vol. 133, no. 5, p. 305.
18. Xu, X., Liao, Y., Yu, G., et al., *Chem. Mater.*, 2007, vol. 19, no. 7, p. 1740.
19. Sano, T., Nishio, Y., Hamada, Y., et al., *J. Mater. Chem.*, 2000, vol. 10, no. 1, p. 157.
20. Wu, X., Hua, Y., Wang, Z., et al., *Optik*, 2006, vol. 117, no. 8, p. 373.
21. Burlov, A.S., Kuznetsova, L.I., Volbushko, N.V., et al., *Russ. J. Gen. Chem.*, 1998, vol. 68, no. 3, p. 463.
22. Minkin, V.I., Tsivadze, A.Yu., Burlov, A.S., et al., RF Patent 2408648, *Byull. Izobret.*, 2011, no. 1.
23. Minaeva, V.A., Minaev, B.F., Baryshnikov, G.V., et al., *Russ. J. Gen. Chem.*, 2011, vol. 81, no. 11, p. 2332.
24. Minaev, B.F., Baryshnikov, G.V., Korop, A.A., et al., *Opt. Spectrosc.*, 2013, vol. 114, no. 1, p. 30.
25. Minaev, B.F., Baryshnikov, G.V., Korop, A.A., et al., *Opt. Spectrosc.*, 2012, vol. 113, no. 3, p. 298.
26. Khan, M.A. and Pinto, A.A., *J. Heterocyclic. Chem.*, 1981, vol. 18, p. 9.
27. SMART (control) and SAINT (integration) Software. Version 5.0, Madison (WI, USA): Bruker AXS Inc., 1997.
28. Sheldrick, G.M., *SADABS. Program for Scanning and Correction of Area Detector Data*, Göttingen (Germany): Univ. of Göttingen, 2003.
29. Sheldrik, G.M., *Acta Crystallogr., Sect. A: Found. Crystallogr.*, 2008, vol. 64, p. 112.
30. Frisch, M.J., Trucks, G.W., Schlegel, H.B., et al., *Gaussian 03. Revision A.1*, Pittsburgh (PA, USA): Gaussian Inc., 2003.
31. Lee, C., Yang, W., and Parr, R.G., *Phys. Rev. B: Condens. Matter*, 1988, vol. 37, p. 785.
32. Becke, A.D., *J. Chem. Phys.*, 1993, vol. 98, no. 7, p. 5648.
33. McLean, A.D. and Chandler, G.S., *J. Chem. Phys.*, 1980, vol. 72, no. 10, p. 5639.
34. Raghavachari, K., Binkley, J.S., Seeger, R., and Pople, J.A., *J. Chem. Phys.*, 1980, vol. 72, no. 1, p. 650.
35. Cornago, P., Escolastio, C., Santa, Maria, M.D., and Claramunt, R.M., *Tetrahedron*, 1996, vol. 52, no. 33, p. 11075.
36. Mahia, J., Maestro, M., Vazquez, M., et al., *Acta Crystallogr., Sect. C: Cryst. Struct. Commun.*, 1999, vol. 55, p. 2158.

Translated by E. Yablonskaya